

Effects of Hydroxyl Group in AlO_x Gate Insulator on the Negative Bias Illumination Instability of In-Ga-Zn-O Thin Film Transistors

Kyoung Woo Park,* Gukjin Jeon, Seunghye Lee, Jong Beom Ko, and Sang-Hee K. Park*

Effects of hydroxyl group (OH) in the gate insulator (GI) of AlO_x formed by atomic layer deposition on the negative bias illumination stress (NBIS) stability of amorphous InGaZnO (a-IGZO) thin film transistors (TFTs) by changing the deposition temperature (T_{dep}) of the AlO_x GI are studied. There are no significant differences in the electrical properties and stabilities of each device, such as field effect mobility (μ_{FE}), subthreshold swing (S.S.), turn on voltage (V_{on}), positive bias temperature stress (PBTS), and negative bias temperature stress (NBTS). Meanwhile, the NBIS stability is improved, resulting in V_{on} shift from -4.34 V to -2.48 V as the T_{dep} of the GI increased. This suggests that as the amount of OH increases in GI, more hole/and or ionized V_{o} trapping sites are formed in the bulk GI. Based on the energy level in photoluminescence (PL) spectra of ALD AlO_x , it is suggested OH related-bulk trapping sites in ALD AlO_x as the origin of non-bridging oxygen hole center (NBOHC) in AlO_x GI.

the amounts of H in the IGZO, determined by effusing from each layer and diffusion into the active layer during the thermal annealing process, is essential to achieving highly stable IGZO TFTs.

In contrast to the PBTS, progress on the negative bias illumination stress (NBIS) stability has been relatively slow. The direct injection and/or trapping of photo-generated holes and/or ionized oxygen vacancies (V_{o}^+ , V_{o}^{2+}), into the gate dielectric bulk have been suggested to be the main mechanisms of NBIS.^[6,7] Intensive studies related to the NBIS instability mechanism have revealed that not only holes but also oxygen vacancies (V_{o}) are related to the NBIS instability.^[6,7] Recently, Jia et al., reported that cation vacancy also a possible reason for NBIS instability.^[8] Unfortunately, the origin of defects in GI which capture the hole and/or ionized oxygen vacancy is neither clearly examined nor fully understood at this moment.

1. Introduction

The electrical stabilities of amorphous indium gallium zinc oxide (a-IGZO) thin film transistors (TFTs) have been astonishingly improved, allowing them to be applied in large size Organic Light Emitting Diode (OLED) TV products and high resolution Liquid Crystal Display (LCD) monitors.^[1] The stability under positive bias temperature stress (PBTS) of a-IGZO TFT, which is the main requirement for a TFT for OLED driving, was achieved by minimizing charge trapping sites in the front and back interfaces, and active layer.^[2,3] Hydrogens (H) in the active layer, gate insulator (GI), passivation layer, and substrate buffer layer are key passivators of these defects.^[4,5] H in the active layer, however, can act as a shallow donor, too. Therefore, controlling

The main trend of TFT-LCD is achieving high resolution TV such as 8 K. Since the off-state time of the switching TFT with light exposure increases along with the increase of the display resolution, obtaining improved stability under NBIS of oxide TFT becomes of importance. Therefore, clarification of the origin of defects in the GI is essential.^[9,10]

According to the first report on the stability of transparent ZnO TFT with wide band-gap of alumina deposited by atomic layer deposition (ALD) at 200°C ,^[11] the PBTS, Positive Bias Illumination Stability (PBIS), and even the NBTS of the ZnO TFT were very good. Only the NBIS, however, was exceptionally poor and its origin has not been clarified yet. We strongly doubt the coinstantaneous and contradictory effect of hydrogen in hydroxyl group in AlO_x GI on the NBIS and PBTS of oxide TFT. It is because alumina deposited by ALD at relatively low temperature contains high amounts of hydrogen as a form of $-\text{OH}$.^[12]


Here, we scrutinized systematically the influence of hydroxyl group in the GI on the NBIS of a-IGZO top gate TFT and the origin of defects in the GI, trapping holes or ionized V_{o} generated in the IGZO film.

2. Experimental Section

We deposited a-IGZO semiconductor with 1:1:1 cation composition using RF sputtering at P_{O_2} of 40% on top of the patterned

K. W. Park, G. Jeon, S. Lee, J. B. Ko, Prof. S.-H. K. Park
Department of Materials Science and Engineering
KAIST
291 Daehak-ro, Yuseong-gu, Daejeon 34141, Republic of Korea
E-mail: ares03011@kaist.ac.kr; shkp@kaist.ac.kr

K. Woo Park, J. B. Ko
Module Development Team
Samsung Display
1 Samsung-ro, Yongin-si, Gyeonggi-do 17113, Republic of Korea

 The ORCID identification number(s) for the author(s) of this article can be found under <https://doi.org/10.1002/pssa.201800737>.

DOI: 10.1002/pssa.201800737

InSnO (ITO) source/drain (SD) electrode, at room temperature. Before the active layer patterning, 10 nm thick AlO_x protection layer was deposited by thermal ALD method using trimethyl-aluminum (TMA) and H_2O precursors.^[13] The protection layer was deposited at temperature of 200 (device a), 250 (device b), and 300 (device c) degrees to control the amount of H and OH in AlO_x . The 20 nm thick 1st GI was deposited to avoid the edge effect on active layer during main GI deposition with same condition of protection layer after simultaneous patterning of the active/protection layer. Then, 100 nm thick AlO_x main GI layer was deposited at 200 °C. A 80 nm thick Mo gate electrode layer was deposited by using DC sputtering method. Finally, all devices were post-annealed at 300 °C in vacuum. Secondary Ion Mass Spectrometry (SIMS, IMS 7F, CAMERA), Fourier Transform Infrared (FT-IR, HYPERION 3000, Bruker) and X-ray Photoelectron Spectroscopy (XPS, K-alpha, Thermo VG Scientific.) were conducted to analyze AlO_x thin films. The TFT properties were measured with Agilent B1500A semiconductor parameter analyzer. The turn on voltage (V_{on}) was determined by the V_{gs} which induced an I_{ds} of $W/L \times 10 \text{ nA}$ at a V_{ds} of 0.1 V. Field effect mobility (μ_{FE}) was characterized at a V_{ds} of 0.1 V in linear region using following equation:

$$\mu_{\text{FE}} = L g_m / W C_i V_{\text{ds}} \quad (1)$$

where the W and L are the channel width and length, respectively. The g_m is the trans-conductance at a low drain voltage, C_i is the capacitance of gate insulator per unit area, and V_{ds} is 0.1 V. PBTS, NBTS, and NBIS reliability were measured for 10 000 s under bias stress of +2, -2, and -2 MV cm^{-1} at 60 °C, respectively. Light irradiation intensity was 0.5 mW cm^{-2} , and a halogen lamp was used as the light source. To measure the photoluminescence (PL) spectra of the AlO_x , we prepared each 100-nm-thick film at different deposition temperatures (T_{dep}) on the glass substrate. PL spectra were measured with HOBIRA QM-400 fluorometer using a 200 nm xenon lamp as an excitation source. The emitted light was collected from the wavelength band ranging from the 250 nm to the 800 nm.

3. Results and Discussion

In a bottom gate structured oxide TFT, charge trapping can easily happen at the front interface between the sputtered oxide semiconductor and GI. This is due to the negative oxygen ion bombardment, which yields not only poor PBTS but also poor NBIS.^[14] To minimize this kind of interface effect and to magnify

the bulk defects of the GI, we fabricated top-gated bottom contact TFTs (TGBC) as shown in **Figure 1**. Furthermore, in the case of the ultra-high resolution display, self-aligned (SA) TFT is considered as the best structure for the reduction of RC delay and TGBC TFT is considered to be able to mimic SA TFT structure in terms of sequence of each layer deposition.

First, we used FT-IR analysis to evaluate the difference of H-related species amounts, such as the OH groups in each AlO_x film. In the FT-IR spectra, the range of 3200–3600 cm^{-1} is related to stretching vibration bond of hydroxyl groups (–OH). However, there was no obvious difference in FT-IR results as shown in **Figure 2(a)**. It means that FT-IR is not suitable in identifying the minute difference of each thin film produced by the same deposition method, due to the resolution limit of FT-IR. So we conducted SIMS analysis for more precise analysis of H-related species amounts in each AlO_x film. As illustrated in **Figure 2(b,c)**, the amount of H and OH contained in the AlO_x film increased as the T_{dep} of AlO_x film decreased. The low T_{dep} interferes with the complete ALD sub-reaction between the surface chemisorbed $\text{Al}(\text{OH})_2$ and TMA due to the steric hindrance of precursors, resulting in unreacted residues of OH in the AlO_x film.^[11] This allowed us to easily control the H content in the AlO_x film by changing T_{dep} .

The transfer characteristics of the TFTs are shown in **Figure 3** and the parameters are summarized in **Table 1**. The channel width (W) and length (L) of the measured TFTs were 40 and 20 μm , respectively. Each device has subthreshold swing (S.S.) value of 0.178 to 0.225 V dec^{-1} , V_{on} of –0.16 to –0.44 V, hysteresis of 0.13 to 0.27 V, and μ_{FE} of 9.6 to 10.55 $\text{V cm}^{-2} \text{ V}^{-1} \text{ s}^{-1}$. While the mobility increases and the S.S decrease as the GI T_{dep} decreases, V_{on} increases as the GI T_{dep} increases.

Although there was no clear trend in terms of the S.S. characteristics among the devices, we expected that H diffused from the GI deposited at the lowest temperature of 200 °C into the interface and/or active layer can passivate the defects, yielding improved mobility and lower V_{on} as reported in previous studies.^[15,16] These indicate that the shallow traps located at the front interface can be controlled quite well by the adoption of AlO_x GI deposited by thermal ALD using water.

To examine the stability of TFTs depending on the H amounts in the AlO_x GI, we measured PBTS, NBTS, and NBIS. **Figure 4** (a–c) shows the evolution of the ΔV_{on} of each TFT as a function of the bias stressing time under each condition. **Figure 4(d)** summarizes the final ΔV_{on} of each TFT after stress time of 10 000 s. While all of the TFTs suffer from slight V_{on} shift within similar range under PBTS and NBTS, the larger instability of

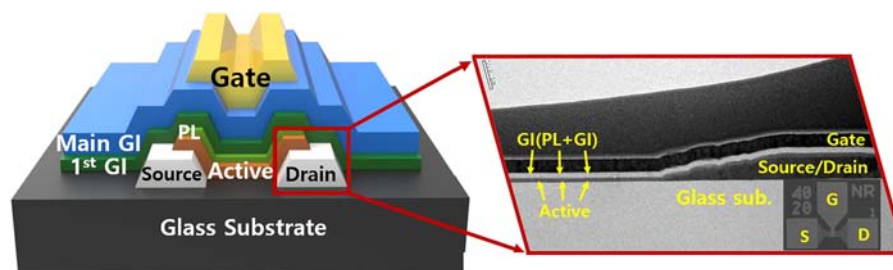


Figure 1. Schematic structure and TEM cross sectional image of a top gate bottom contact IGZO TFT.

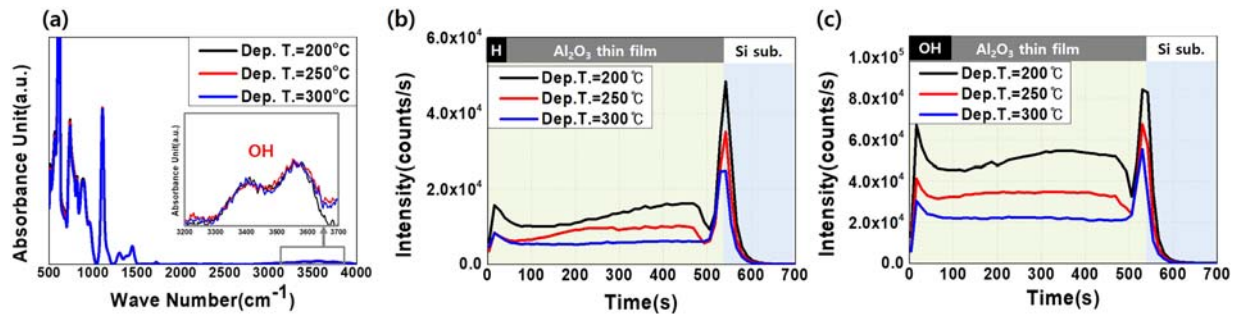


Figure 2. Analysis results of the (a) FT-IR and SIMS depth profile for the amount of (b) hydrogen and (c) hydroxide in AlO_x deposited at different temperatures.

device A with the GI of alumina deposited at the lowest temperature became clearer under the NBIS condition. We illuminated light through the Mo metal gate electrode and the effective light intensity illuminated onto the active layer was weaker than 0.5 mW cm^{-2} . While the IGZO TFT with AlO_x GI with smallest amount of OH showed -2.38 V shift after 10 000 s stress, the one with the GI containing largest amount of OH showed the largest negative V_{on} shift of -4.62 V . The application of GI with lower content of OH and H improved photo-stability under negative bias stress for IGZO TFT.

In oxide semiconductors such as IGZO, formation enthalpy (ΔH) of ionized V_{O} (V_{O}^+ or V_{O}^{2+}) is smaller than that of neutral V_{O} , and the holes generated by light illumination can be easily captured by the V_{O} , resulting in deteriorated S.S. characteristics after NBIS.^[17] In our case, however, the change of S.S. of each TFT a, b, and c during the NBIS were 0.018, 0.044, and 0 V dec^{-1} , as shown in Figure 5(a–c), respectively. These negligible changes of S.S. of each TFT implied that the ionized V_{O} located below the mid-gap of IGZO. Also, the transfer curve was shifted to a negative direction without the changing of S.S. value during the NBIS test, indicating that another new defect generation did not occur. In addition, the degree of injection or trapping of holes and/or ionized V_{O} is quite dependent on the inherent defects in both IGZO and GI layers.

It was reported that the Metal-H can play as the hole trapping center in IGZO semiconductor.^[6] The amount of H in IGZO in our TFT could be different in spite of the same deposition condition of IGZO because the amount of H diffused from AlO_x into the active layer was different. Nonetheless, in this experiment, we just focus on the trapping of positive charged species only in the GI layer.

The trapping model under NBIS of oxide TFT was mainly illustrated by the valence band off set between the oxide semiconductor and GI. The V_{on} shift under the NBIS of IGZO TFT with SiN_x GI of which band offset with IGZO is about 0.15 eV showed V_{on} shift larger than -10 V . Meanwhile that with SiO_2 having offset of 2.8 eV with IGZO was only 2.1 V.^[18] Our device c with AlO_x deposited at 300°C showed a negative shift comparable to that of PECVD SiO_2 . However, device A with the AlO_x containing relatively larger amount of OH showed an increased negative shift. However, it was still much smaller than that with SiN_x . From these previous results, it is quite reasonable to ascribe the NBIS instability of IGZO TFT a, b, c to the hole and/or ionized V_{O} trap into the bulk states of the AlO_x GI with band gap ranging from 6.65 to 6.95 eV.^[19] The huge negative shift, reported from ZnO TFT with ALD AlO_x GI deposited at 200°C ,^[10] could be attributed to the combined effects of the intense light illumination through the transparent ITO electrode, more V_{O} in the ALD grown ZnO active layer, and the trapping sites in the AlO_x GI.

Tsubuku et al. suggested non-bridging oxygen hole center (NBOHC) in SiO_x film as the main origin of the trapping center.^[20] This can be generated by either a rupture of strained Si–O–Si bond or breaking of the silanol group, Si–O–H to give Si–O· + ·H. It was reported that silica with high density of H contains larger number of NBOHC than that with less H. The

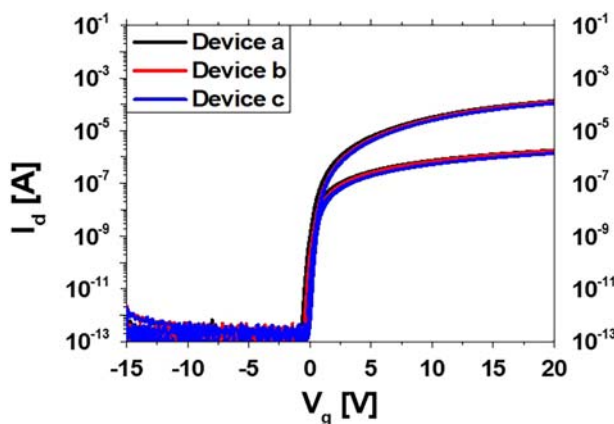


Figure 3. Transfer curves of device a, device b, and device c.

Table 1. Parameters of each TFT depending on the T_{dep} of the AlO_x gate insulator.

Device	S.S. [V dec^{-1}]	V_{on} [V]	Hysteresis [V] @ $V_{\text{ds}} = 0.1 \text{ V}$	μ_{lin} [$\text{cm}^2/\text{V}^{-1} \text{ s}^{-1}$]
a	0.209	−0.44	0.13	10.34
b	0.178	−0.3	0.27	10.55
c	0.225	−0.16	0.13	9.65

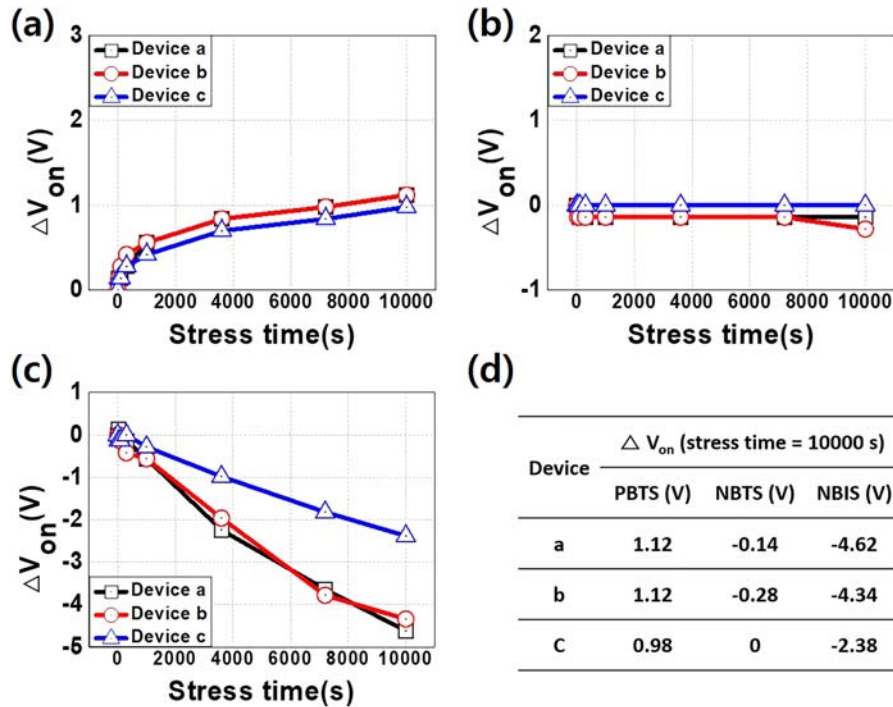


Figure 4. Results of (a) PBTS, (b) NBTS, and (c) NBIS reliabilities in each device. d) And summary of ΔV_{on} in each device after various stress.

energy level of NBOHC located at the deep level has been confirmed by the first-principle calculation and PL.^[21,22]

AlO_x deposited by ALD using water also contains $AlO(OH)_x$ depending on the process temperature.^[12] Furthermore, H from OH groups can easily dissociate and diffuse out during the thermal annealing at a temperature higher than the T_{dep} , and act as the passivator of defects at the interface and oxide semiconductor of oxide TFT.^[23] Then the remaining Al-O acts as an NBOHC at relatively deep level, resulting in the negative V_{on} shift under NBIS by trapping the holes or/and ionized V_o . To identify the defects in AlO_x films, we measured PL of AlO_x GI films using 200 nm xenon lamp as an excitation source. **Figure 6** (a) illustrates PL spectra of the AlO_x films deposited at 200, 250, and 300 °C. Characteristic of excitation source peaks at 400 nm, and other peaks were observed in all AlO_x films.

According to the PL of boehmite, aluminum oxide hydroxide powders ($\gamma-AlO(OH)$) prepared by the sol-gel process using aluminum alkoxide, F^+ center and NBOHC ($=Al-O\cdot$) contributed to the PL at 440 nm, and 624, 664 nm, respectively.^[24,25] The PL emission can be shifted depending on the surface, powder size, or film thickness. Since AlO_x containing OH group deposited by ALD has a structure similar to the boehmite, the PL emission peak around at 649 nm could be assigned to the origin of NBOHC, $OH\cdot$, in the AlO_x films. This peak is originated from the 1) transition of electron from the valence band or/and states of alumina to the conduction band by the light illumination; 2) then trapping to the states within the band gap; 3) followed by the transition to the valence band of alumina, to emit the light corresponding to the PL at 649 nm. Although the PL emission peak position can be affected by the

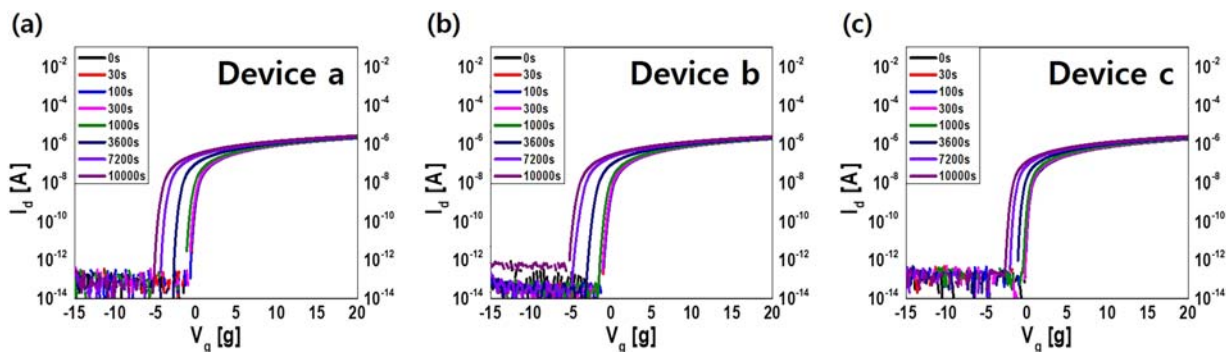


Figure 5. Transfer curves of the (a) device a, (b) device b, and (c) device c under NBIS conditions.

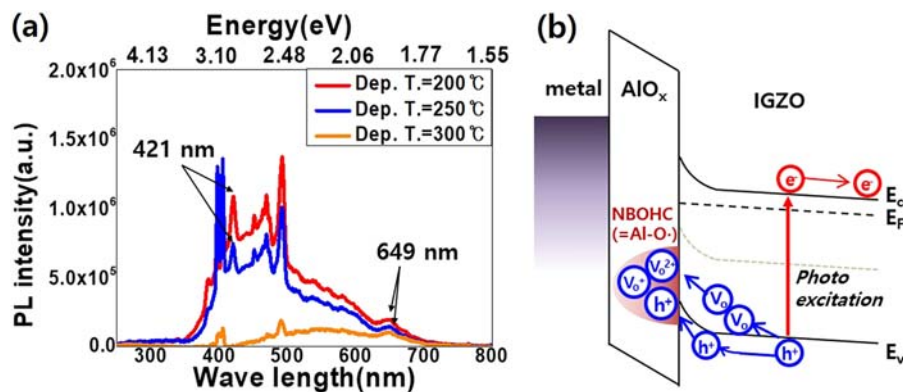


Figure 6. a) Emission spectra for AlO_x films detected at 200 nm excitation wave length. b) Model for trapping of hole/ionized V_o of IGZO film in the OH related bulk trap in AlO_x films.

excitation source, the PL of the NBOHC peak in SiO_2 is also reported to be around 650 nm.^[22]

Based on the PL peaks of each AlO_x film and the degree of the V_on shift of IGZO TFT a, b, and c under NBIS, we suggest a plausible band diagram showing the trapping process for hole and ionized V_o into the hydroxyl related traps in AlO_x as shown in Figure 6(b). Although the band offset between the IGZO and ALD grown AlO_x is not clear yet, this mechanism is consistent with the NBIS instability of IGZO TFT with the wide band gap AlO_x GI.

4. Conclusion

We investigated the effect of H and OH in the AlO_x GI by ALD on the NBIS stability of *a*-IGZO TFTs. We found that TFT with larger OH amount AlO_x showed larger negative V_on shift under NBIS without significant S.S. deterioration. According to the PL spectra, ALD AlO_x films have OH related NBOHC at around 1.91 eV above the valence band, similar to the energy level of NBOHC in SiO_2 film. The AlO_x film with largest amount of OH shows highest PL peak at 649 nm.

These results indicate that the H in ALD AlO_x stacked *a*-IGZO TFT show inextricably instantaneous and contradictory effect: One thing is to passivate the defects in the channel-interface of TFT as reported previously and the other is to generate NBOHC in the AlO_x to result in NBIS instability. Here, we presented the first finding of the origin of hole and/or ionized V_o defects trapping sites in ALD AlO_x film.

Acknowledgements

This research was funded by Samsung Display Corporation through KAIST Samsung Display Research Center Program and by Wearable Platform Materials Technology Center (WMC) funded by the National Research Foundation of Korea (NRF) Grant of the Korean Government (MSIP) (No. 2016R1A5A1009926).

Conflict of Interest

The authors declare no conflict of interest.

Keywords

amorphous InGaZnO , hydrogen, negative bias illumination stress instability, non-bridging oxygen hole center, thin film transistors

Received: September 20, 2018
Revised: November 29, 2018
Published online: January 18, 2019

- [1] J. Y. Kwon, J. K. Jeong, *Semicond. Sci. Technol.* **2015**, *30*, 024002.
- [2] A. Suresh, J. F. Muth, *Appl. Phys. Lett.* **2008**, *92*, 033502.
- [3] J.-M. Lee, I.-T. Cho, W.-S. Cheong, C.-S. Hwang, H.-I. Kwon, *Appl. Phys. Lett.* **2009**, *94*, 222112.
- [4] Y. Nam, H.-O. Kim, S. H. Cho, C.-S. Hwang, H. Kim, S. Jeon, S.-H. K. Park, *J. Inf. Disp.* **2016**, *17*, p1.
- [5] Y. Hanyu, D. Domen, K. Nomura, H. Hiramatsu, H. Kumomi, H. Hosono, T. Kamiya, *Appl. Phys. Lett.* **2013**, *103*, 202114.
- [6] J. Bang, S. Matsuishi, H. Hosono, *Appl. Phys. Lett.* **2017**, *110*, 232105.
- [7] M. P. Hung, D. Wang, T. Toda, J. Jiang, M. Furuta, *ECS J. Solid State Sci. Technol.* **2014**, *3*, Q3023.
- [8] J. Jia, A. Suko, Y. Shigesato, *Phys. Rev. Appl.* **2018**, *9*, 014018.
- [9] M. Li, L. Lan, M. Xu, L. Wang, H. Xu, D. Luo, J. Zou, H. Tao, R. Yao, J. Peng, *J. Phys. D: Appl. Phys.* **2011**, *44*, 455102.
- [10] D.-G. Yang, H.-D. Kim, J. H. Kim, K. Park, J.-H. Kim, Y. J. Kim, J. Park, H.-S. Kim, *J. Alloys Compd.* **2017**, *729*, 1195.
- [11] J.-H. Shin, J.-S. Lee, C.-S. Hwang, S.-H. K. Park, W.-S. Cheong, M. K. Ryu, C.-W. Byun, J.-I. Lee, H. Y. Chu, *ETRI J.* **2009**, *31*, p62.
- [12] S. J. Yun, K.-H. Lee, J. Skarp, H.-R. Kim, K.-S. Nam, *J. Vac. Sci. Technol. A* **1997**, *15*, p2993.
- [13] S.-H. K. Park, D.-H. Cho, C.-S. Hwang, S. Yang, M. K. Ryu, C.-W. Byun, S. M. Yoon, W.-S. Cheong, K. I. Cho, J.-H. Jeon, *ETRI J.* **2009**, *31*, p653.
- [14] S.-H. Cho, M. K. Ryu, H.-O. Kim, O.-S. Kwon, E.-S. Park, Y.-S. Roh, C. S. Hwang, S.-H. K. Park, *Phys. Status Solidi A* **2014**, *211*, p2126.
- [15] Y. Hanyu, D. Domen, K. Nomura, H. Hiramatsu, H. Kumomi, H. Hosono, T. Kamiya, *Appl. Phys. Lett.* **2013**, *103*, 202114.
- [16] S. W. Tsao, T. C. Chang, S. Y. Huang, M. C. Chen, S. C. Chen, C. T. Tsai, Y. J. Kuo, Y. C. Chen, W. C. Wu, *Solid-State Electron.* **2010**, *54*, 1497.
- [17] P. Miglitoro, J. Jang, *Handb. Visual Disp. Technol.* **2016**, p1018.
- [18] S. Miyazaki, M. Hirose, *AIP Conf. Proc.* **2001**, *550*, p89.

- [19] M. L. Huang, Y. C. Chang, C. H. Chang, T. D. Lin, J. Kwo, T. B. Wu, M. Hong, *Appl. Phys. Lett.* **2006**, 89, p1.
- [20] M. Tsubuku, R. Watanabe, N. Isihara, H. Kishida, M. Takahashi, S. Yamazaki, Y. Kanzaki, H. Matsukizono, S. Mori, T. Matsuo, *SID DIGEST* **2013**, 16.1, p166.
- [21] M. Benoit, M. Pohlmann, W. Kob, *Europhys. Lett.* **2008**, 82, p1.
- [22] S. Munekuni, T. amanaka, Y. Shimogaichi, R. Tohmon, Y. Ohki, K. Nagasawa, Y. Hama, *J. Appl. Phys.* **1990**, 68, p1212.
- [23] Y. Nam, H.-O. Kim, S. H. Cho, S.-H. K. Park, *RSC Adv.* **2018**, 8, p5622.
- [24] Z. Q. Yu, C. X. Wang, X. T. Gu, C. Li, *J. Lumin.* **2004**, 106, 153.
- [25] H. Hou, Y. Xie, Q. Yang, Q. Guo, C. Tan, *Nanotechnology* **2005**, 16, 741.